Supplementary Material

Dual-phased $Mo_2C/Mo_3N_2/C$ nanosheets for efficient electrocatalytic hydrogen evolution

Guangyan Tian,[a,c,#] Bingxue Yao,[a,#] Gaofeng Han,[b,*] Yan Li,[a] Kefeng Zhang,[a] and Junping Meng[a*]

[a]Key laboratory of special Functional Materials for Ecological Environment and Information, Hebei University of Technology, Ministry of Education, Tianjin 300130, P.R. China.

[b]School of Materials Science and Engineering, Tianjin Chengjian University, Tianjin 300384, P.R. China.

[c]School of Materials Science and Engineering, Hebei University of Technology, Tianjin 300130, P.R. China.

[#]Co-first author.

Corresponding author: Email: hangaofeng@tcu.edu.cn; mengjunping@hebut.edu.cn

Supporting discussion

Based on the linear fitting of Figure 4d and Figure 5c, we can obtain its specific capacitance as follows:

(Where C_{dl} is the fitting slope, m is the catalyst loading mass. we can calculate its ECSA by assuming a standard value of 40 μF/cm^2).

Under 1M KOH condition:

$$ECSA_{(Carbon)} = \frac{Cdl}{m} \times \frac{1}{40\ \mu F\ cm^{-2}} = \frac{6.67\ mF\ cm^{-2}}{1.42\ mg\ cm^{-2}} \times \frac{1}{0.04\ mF\ cm^{-2}} \approx 117.43\ cm^2\ mg^{-1}$$

$$ECSA_{(Mo2C/C)} = \frac{Cdl}{m} \times \frac{1}{40\ \mu F\ cm^{-2}} = \frac{50.44\ mF\ cm^{-2}}{1.42\ mg\ cm^{-2}} \times \frac{1}{0.04\ mF\ cm^{-2}} \approx 888.03\ cm^2\ mg^{-1}$$

$$ECSA_{(Mo3N2/C)} = \frac{Cdl}{m} \times \frac{1}{40\ \mu F\ cm^{-2}} = \frac{20.31\ mF\ cm^{-2}}{1.42\ mg\ cm^{-2}} \times \frac{1}{0.04\ mF\ cm^{-2}} \approx 357.57\ cm^2\ mg^{-1}$$

$$ECSA_{(Mo2C/Mo3N2/C)} = \frac{Cdl}{m} \times \frac{1}{40\ \mu F\ cm^{-2}} = \frac{94.92\ mF\ cm^{-2}}{1.42\ mg\ cm^{-2}} \times \frac{1}{0.04\ mF\ cm^{-2}} \approx 1671.13\ cm^2/mg$$

Under 0.5M H_2SO_4 condition:

$$ECSA_{(Carbon)} = \frac{Cdl}{m} \times \frac{1}{40\ \mu F\ cm^{-2}} = \frac{4.76\ mF\ cm^{-2}}{1.42\ mg\ cm^{-2}} \times \frac{1}{0.04\ mF\ cm^{-2}} \approx 83.80\ cm^2\ mg^{-1}$$

$$ECSA_{(Mo2C/C)} = \frac{Cdl}{m} \times \frac{1}{40\ \mu F\ cm^{-2}} = \frac{29.38\ mF\ cm^{-2}}{1.42\ mg\ cm^{-2}} \times \frac{1}{0.04\ mF\ cm^{-2}} \approx 517.25\ cm^2\ mg^{-1}$$

$$ECSA_{(Mo3N2/C)} = \frac{Cdl}{m} \times \frac{1}{40\ \mu F\ cm^{-2}} = \frac{14.39\ mF\ cm^{-2}}{1.42\ mg\ cm^{-2}} \times \frac{1}{0.04\ mF\ cm^{-2}} \approx 253.35\ cm^2\ mg^{-1}$$

$$ECSA_{(Mo2C/Mo3N2/C)} = \frac{\mathrm{Cdl}}{\mathrm{m}} \times \frac{1}{40\ \mu F\ cm^{-2}} = \frac{76.35\ \mathrm{mF\ cm^{-2}}}{1.42\ \mathrm{mg\ cm^{-2}}} \times \frac{1}{0.04\ mF\ cm^{-2}} \approx 1344.19\ cm^2/mg$$

The TOF value is obtained by following equation:

$$TOF = \frac{J \times A}{N \times F \times n} \quad (1)$$

(Where J is the measured current density, A is geometric area of the electrode, N is the number of electrons required for reaction, F is Faraday constant and n is the number of active sites)[1].

DFT Calculations

All the density functional theory (DFT) calculations were carried out using Vienna Ab-initio Simulation Package (VASP)[2], employing the Projected Augmented Wave (PAW) method[3]. As has been proved effective, the revised Perdew-Burke-Ernzerhof (RPBE) functional was used to treat the exchange and correlation effects. The surface of Mo_2C/Mo_3N_2 with ~15 Å vacuum was simulated to represent the catalytic interface. The K points meshing for Brillioun zone was set up as a 3×3×1 grid centered at the gamma point regarding Monkhorst Pack Scheme for geometric optimization of the slab surfaces. All atoms are fully relaxed, the total energy change is less than 10^{-5} eV, the force on each ion is less than 0.02eV/Å. A cutoff energy of 450 eV is set and the forces were converged to 0.02 eV/Å for all calculations. Adsorption energy was calculated by subtracting the energies of gas phase species and clean surface from the total energy of the absorbed system:

$$\Delta GH^{*} = \Delta EH + \Delta EZPE - T\Delta SH \quad (2)$$

where ΔEH is the binding energy of hydrogen atom, $\Delta EZPE$ is the difference in zero-point energy between the adsorbed hydrogen and the gaseous hydrogen gas, and

$T\Delta S_H$ is the entropy difference for the two states. We have calculated a 0.30 eV value in this work to stand for the contribution of zero-point energy and entropy. And a more negative indicates a more stable adsorption.

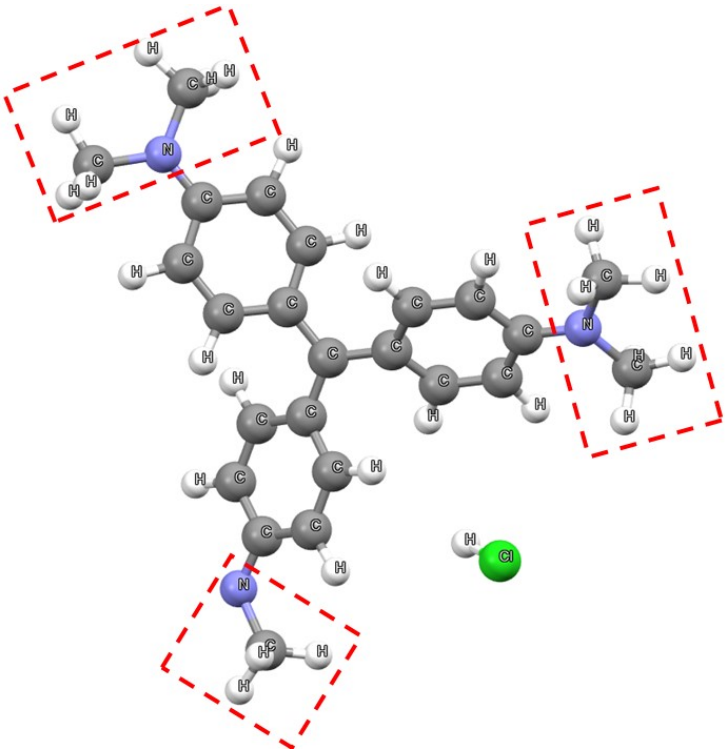

Figure S1. Molecular structure of methyl violet

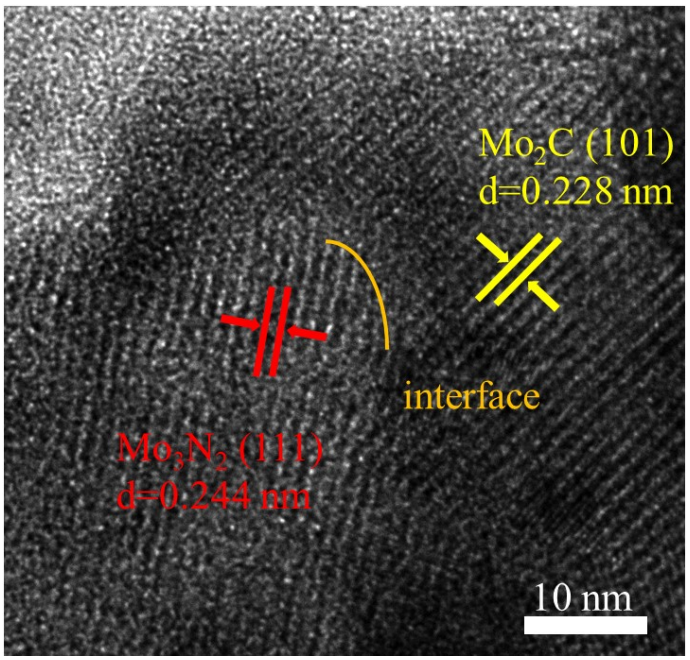

Figure S2. HRTEM image of $Mo_2C/Mo_3N_2/C$

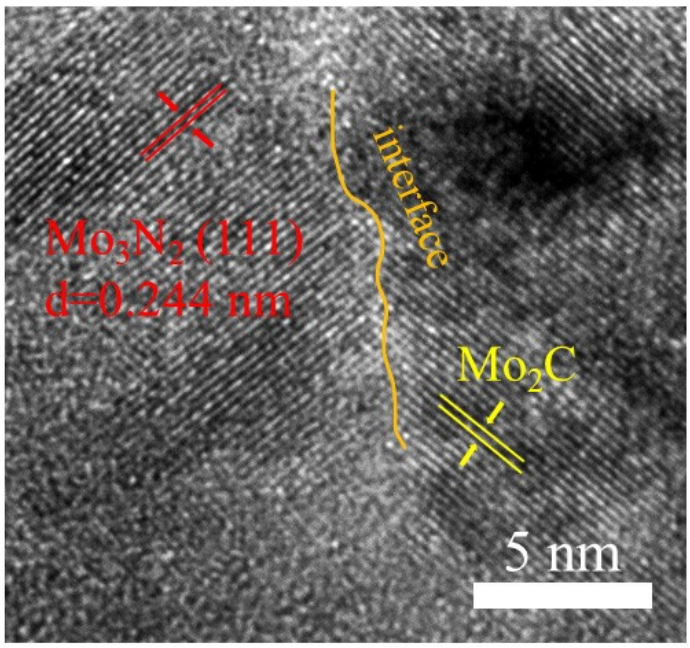

Figure S3. HRTEM image of $Mo_2C/Mo_3N_2/C$

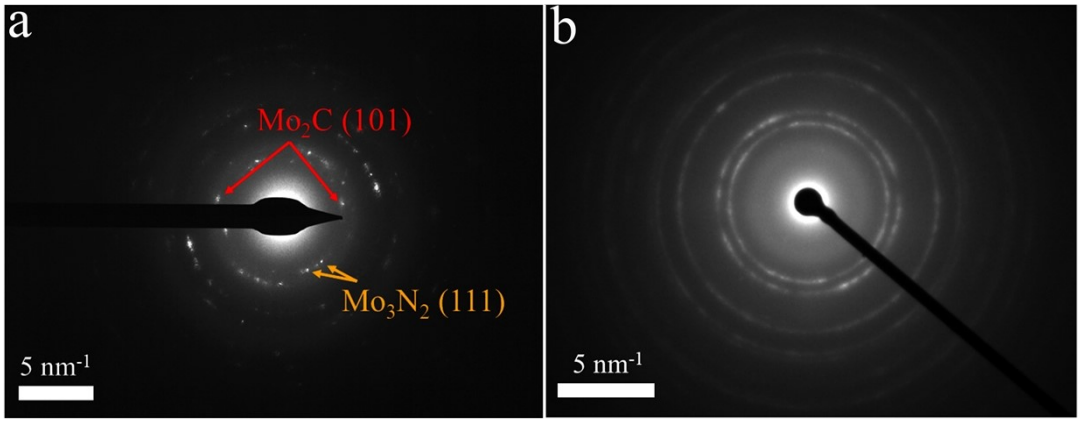

Figure S4. (a, b) SAED pattern of $Mo_2C/Mo_3N_2/C$

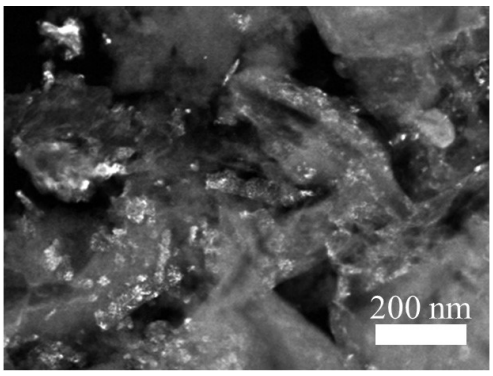

Figure S5. HAADF-STEM micrograph of $Mo_2C/Mo_3N_2/C$.

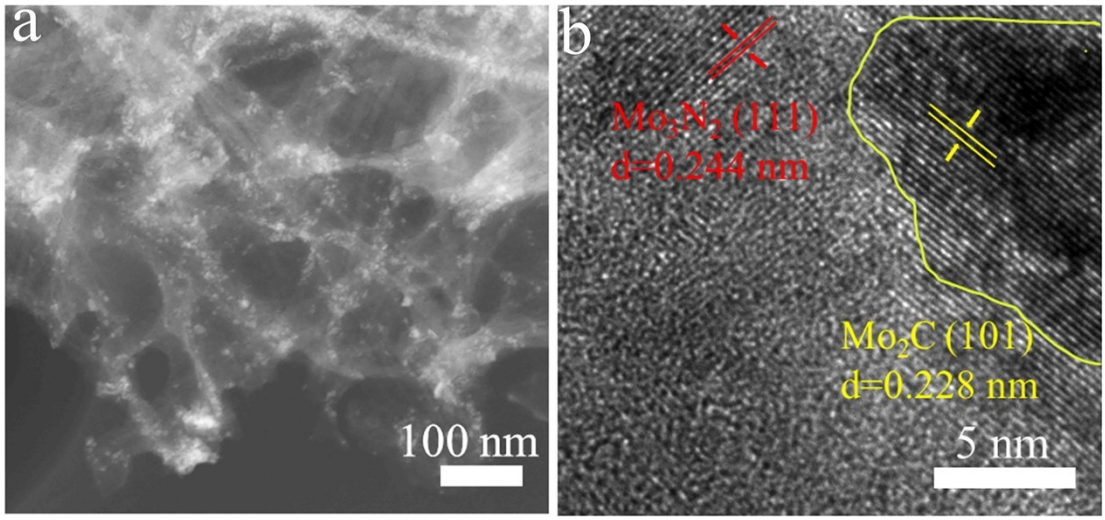

Figure S6. (a) TEM image of $Mo_2C/Mo_3N_2/C$. (b) HRTEM image of $Mo_2C/Mo_3N_2/C$

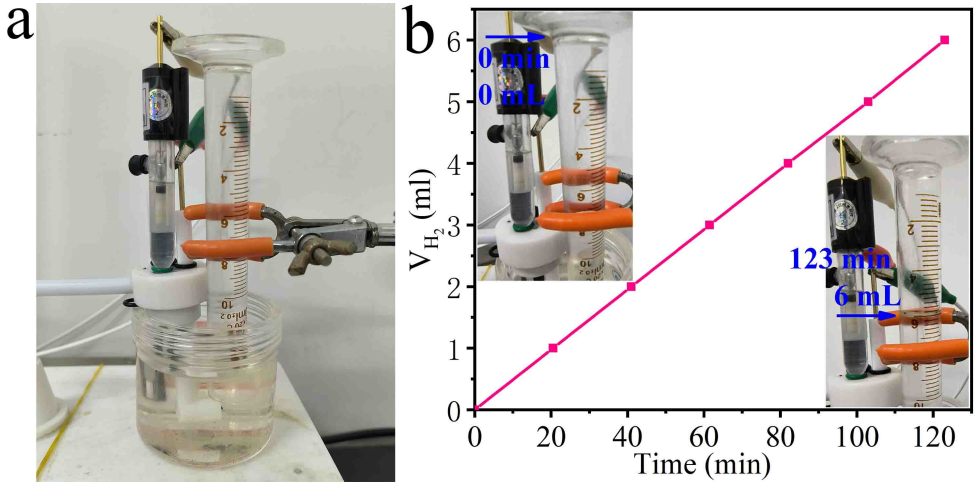

Figure S7. (a) Experimental device, (b) the experimental data of the Faradaic efficiency at 100 mA/cm^2 in 1 M KOH of $Mo_2C/Mo_3N_2/C$

The Faradaic efficiency (FE) was obtained according to Figure S7 (b):

$$FE = \frac{\frac{V(H2)}{Vm}}{\frac{I \times t}{2 \times F}} \times 100\% = \frac{\frac{6 \times 10^{-3}\ L}{22.4\ L/mol}}{\frac{7 \times 10^{-3}\ A \times 7385\ s}{2 \times 96485\ C/mol}} \times 100\% \approx 100\%$$

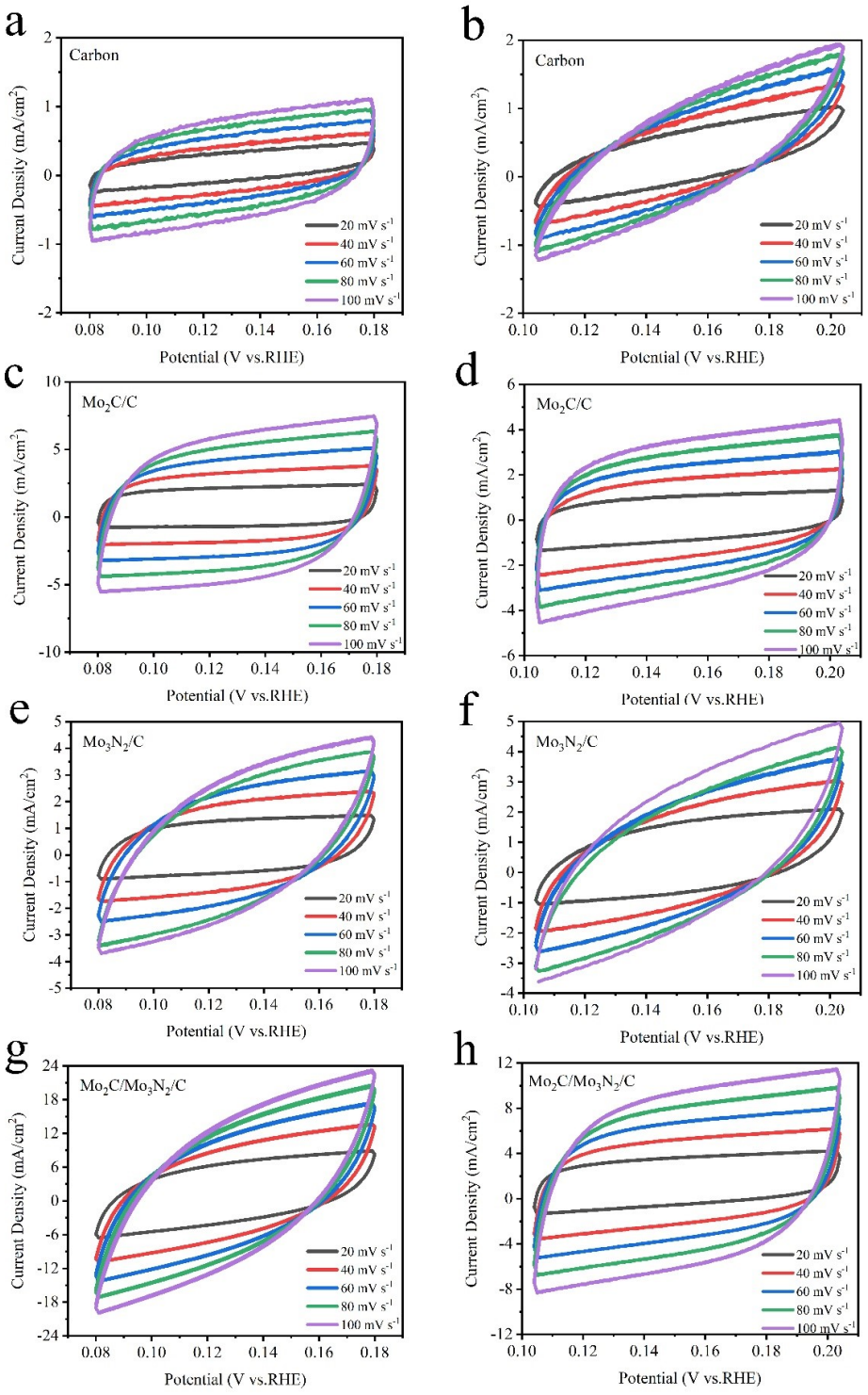

Figure S8. Typical cyclic voltammograms of (a) Carbon, (b) Mo_2C/C, (c) Mo_3N_2/C, and (d) $Mo_2C/Mo_3N_2/C$ with scan rates ranging from 20 mV/s to 100 mV/s under 1 M KOH conditions. Typical cyclic voltammograms of (e) Carbon, (f) Mo_2C/C, (g) Mo_3N_2/C and (h) $Mo_2C/Mo_3N_2/C$ with scan rates ranging from 20 mV/s to 100 mV/s under 0.5 M H_2SO_4 conditions.

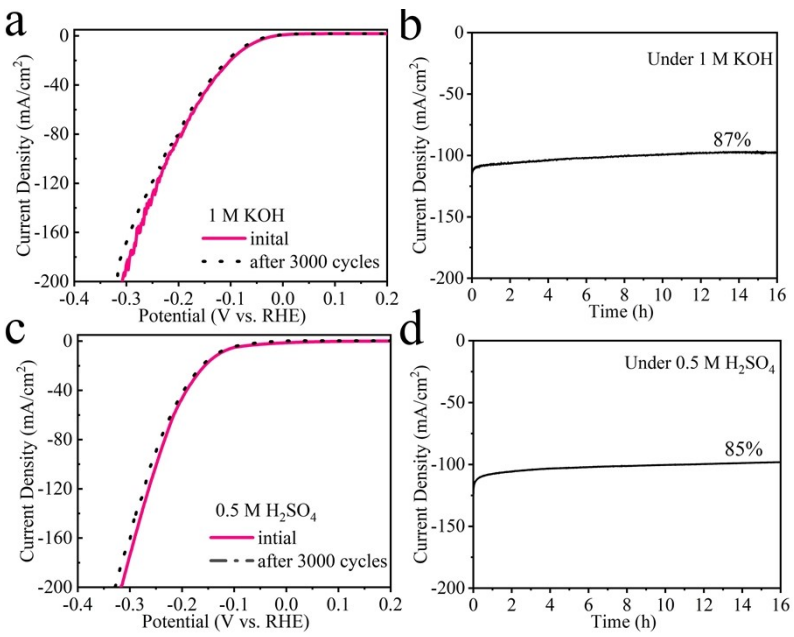

Figure S9. (a) The LSV curves of $Mo_2C/Mo_3N_2/C$ before and after 3000 CV cycles and (b) Chronoamperometry curve of $Mo_2C/Mo_3N_2/C$ under 1 M KOH; (c) The LSV curves of $Mo_2C/Mo_3N_2/C$ before and after 3000 CV cycles and (d) Chronoamperometry curve of $Mo_2C/Mo_3N_2/C$ under 0.5 M H_2SO_4.

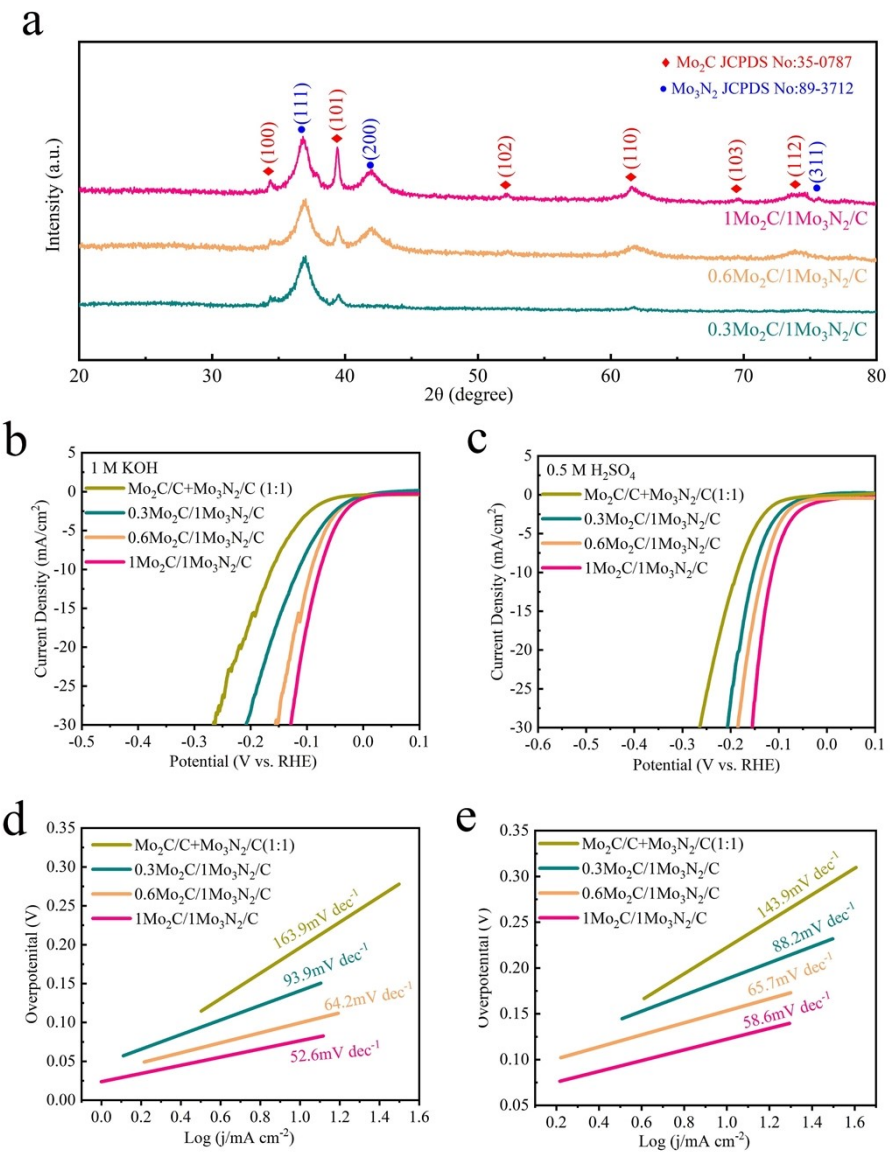

Figure S10. (a) XRD patterns of $Mo_2C/Mo_3N_2/C$ with different ratio of Mo_2C and Mo_3N_2. b, c) Polarization curves and d, e) corresponding Tafel slopes of $0.3Mo_2C/1Mo_3N_2/C$, $0.6Mo_2C/1Mo_3N_2/C$, $1Mo_2C/1Mo_3N_2/C$ and $Mo_2C/C+Mo_3N_2/C$ (1:1).

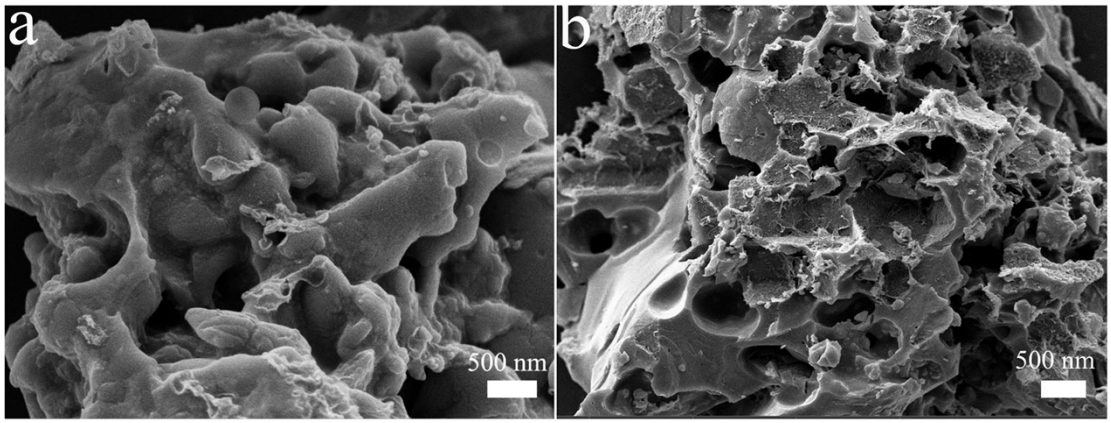

Figure S11. SEM image of $0.3Mo_2C/1Mo_3N_2/C$ (a), $0.6Mo_2C/1Mo_3N_2/C$ (b)

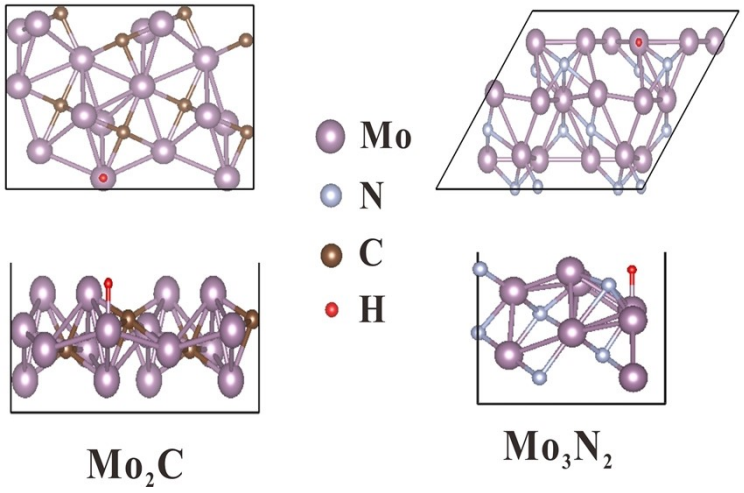

Figure S12. Sites for H_{ads} adsorption on the surface of Mo_2C (a) and Mo_3N_2 (b)

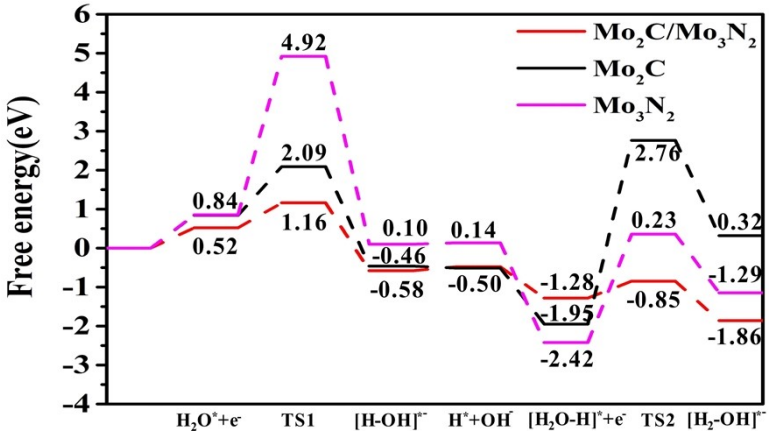

Figure S13. Relative energy profiles (TS-Transition State) of Mo_2C/Mo_3N_2, Mo_2C and Mo_3N_2

Table S1. Comparison of the HER performance of $Mo_2C/Mo_3N_2/C$ with Mo-based electrocatalysts of 10 mA/cm^2 in alkaline conditions.

Catalysts	Support	Loading (mg/cm^2)	Electrolyte	Overpotential (mV)	Tafel Slope (mV/dec)	C_{dl} (mF/cm^2)	Ref.
Hierarchical β-Mo_2C nanotubes	Glassy carbon	0.75	0.1M KOH	112	55	—	[5]
h-Mo_2C/MoO_2	Glassy carbon	0.57	1M KOH	94.7	56.6	139	[6]
Ni/Mo_2C-PC	Glassy carbon	0.5	1M KOH	179	145	11.2	[7]
0.2rGo-MoS_2	Glassy carbon	0.097	1M KOH	314	80	14.67	[8]
Mo_3N_2@NC	Glassy carbon	0.5	1M KOH	85	48.9	60.2	[9]
β-Mo_2C@NPCC	Glassy carbon	0.1	1M KOH	132	49	50	[10]
N,P-Mo_xC NF	Glassy carbon	0.265	1M KOH	135	57.1	51.4	[11]
$Co_{0.60}Mo_{0.40}S_x$	Glassy carbon	0.2	1M NaOH	167	87	—	[12]
Ni/Mo_2C-NCNFs	Glassy carbon	1.4	1M KOH	143	57.8	29.41	[13]
MoC-Mo_2C-31.4 HNWs	Glassy carbon	0.14	1M KOH	120	42	—	[14]
Fe-doped Co-Mo-S/NF	Ni foam	4	1M KOH	105	50.3	—	[15]
Mo_2C/C	Glassy carbon	1.42	1M KOH	142	115.4	50.44	This work
Mo_3N_2/C	Glassy carbon	1.42	1M KOH	187	145.6	20.31	This work
Dual-phased $Mo_2C/Mo_3N_2/C$	Glassy carbon	1.42	1M KOH	76	52.6	94.92	This work

Table S2. Comparison of ECSA of HER electrocatalysts under 1 M KOH or and 0.5 M H_2SO_4 conditions

electrocatalyst	1 M KOH (cm^2/mg)	0.5 M H_2SO_4 (cm^2/mg)
Carbon	117.43	83.80
Mo_2C/C	888.03	517.25
Mo_3N_2/C	357.57	253.35
Mo_2C/Mo_3N_2/C	1671.13	1344.19

Table S3. Comparison of the HER performance for $Mo_2C/Mo_3N_2/C$ catalyst with Mo-based electrocatalysts of 10 mA/cm^2 in acidic condition.

Catalysts	Support	Loading (mg/cm^2)	Electrolyte	Overpotential (10mA/cm^2)	Tafel Slope (mV/dec)	C_{dl} (mF/cm^2)	Ref.
N,P(S)-Mo_2C/C	Glassy carbon	0.213	0.5M H_2SO_4	210 (223)	64 (44)	—	[16]
Mo_2C@C	Glassy carbon	—	0.5M H_2SO_4	170	58	20.2	[17]
MoC-Mo_2C-790	Ni foam	—	0.5M H_2SO_4	114	62	—	[18]
0.2rGo-MoS_2	Glassy carbon	0.097	0.5M H_2SO_4	146	51	14.67	[8]
Mo_3N_2@NC	Glassy carbon	0.5	0.5M H_2SO_4	129	86.7	62.4	[9]
Mo_2C-WC/NCAs	Glassy carbon	1.07	0.5M H_2SO_4	126	72	101	[19]
N,P-Mo_xC NF	Glassy carbon	0.265	0.5M H_2SO_4	107	65.1	38.3	[11]
Mo_2C/NCF	Glassy carbon	0.28	0.5M H_2SO_4	144	55	28.7	[20]
Ni/Mo_2C-NCNFs	Glassy carbon	1.4	0.5M H_2SO_4	195	77.8	—	[13]
MoC-Mo_2C-31.4 HNWs	Glassy carbon	0.14	0.5M H_2SO_4	126	43	6.68	[14]
$FeN_{0.023}/Mo_2C$/C	Glassy carbon	0.25	0.5M H_2SO_4	76	65.2	5.32	[21]
Mo_2C/C	Glassy carbon	1.42	0.5M H_2SO_4	164	102.2	29.38	This work
Mo_3N_2/C	Glassy carbon	1.42	0.5M H_2SO_4	249	124.2	14.39	This work
Dual-phased $Mo_2C/Mo_3N_2/C$	Glassy carbon	1.42	0.5M H_2SO_4	121	59.4	76.36	This work

Table S4. Comparison of the lattice parameters of Mo_2C/Mo_3N_2 before and after structural optimization

The lattice parameters before optimization					
a	b	c	alpha	beta	gamma
10.17720	9.63150	20.44738	81.2960	90.00000	90.0000
The lattice parameters after optimization					
a	b	c	alpha	beta	gamma
10.17720	9.63150	20.44738	81.2960	90.0000	90.0000

Table S5. Comparison of atomic coordinates of Mo_2C/Mo_3N_2 before and after structural optimization

	Atomic coordinates before optimization			**Atomic coordinates after optimization**		
site	X	Y	Z	X	Y	Z
Mo1	1.83660053	7.411181947	1.779276731	1.83660053	7.411181947	1.779276731
Mo2	1.000090945	3.813931133	1.047299804	1.000090945	3.813931133	1.047299804
Mo3	2.387369574	6.789950573	4.141389802	2.387369574	6.789950573	4.141389802
Mo4	3.40261064	9.81192425	3.426547192	3.40261064	9.81192425	3.426547192
Mo5	1.000090945	9.649132685	4.082249369	1.000090945	9.649132685	4.082249369
Mo6	1.83660053	3.123135497	3.350272593	1.83660053	3.123135497	3.350272593
Mo7	3.40261064	4.417228707	1.703002282	3.40261064	4.417228707	1.703002282
Mo8	2.387369574	0.915017641	0.988159597	2.387369574	0.915017641	0.988159597
Mo9	0.950591699	8.103180924	6.261444896	0.935295006	8.089854226	6.254346671
Mo10	0.804364799	5.160955968	5.818057602	0.798505644	5.158648716	5.81583007
Mo11	2.800002812	7.558313627	8.296101425	2.797020422	7.586745262	8.289173066
Mo12	3.110006401	9.813495452	6.871402553	3.125875277	9.82169344	6.807156506
Mo13	0.922966903	10.03551522	8.126766827	0.932148528	9.874271468	8.124778433
Mo14	2.084598729	4.218440141	7.825484991	2.10326862	4.118570113	7.74421501
Mo15	3.55945895	5.54540026	6.298566012	3.557960627	5.5465968	6.297357676
Mo16	2.8412995	2.78139994	5.862607037	2.837187605	2.779481156	5.856874967
Mo17	8.358587698	1.201790883	7.290471318	8.358715693	1.193704116	7.297276796
Mo18	6.20495496	10.30183525	4.85785457	6.192772444	10.29985061	4.859035499
Mo19	6.413431106	2.173053728	1.56583724	6.413431106	2.173053728	1.56583724
Mo20	8.7983976	1.395939365	4.703752183	8.797366973	1.394335306	4.701671928
Mo21	6.413431106	4.580928789	1.56583724	6.413431106	4.580928789	1.56583724
Mo22	9.673490892	3.677558875	3.947229486	9.673490892	3.677558875	3.947229486
Mo23	5.146205513	7.470653536	7.127294057	5.145554016	7.464363075	7.126021268
Mo24	8.659464863	3.72033312	1.79659522	8.659464863	3.72033312	1.79659522

Mo25	7.651637159	8.453349553	6.540591762	7.651510377	8.456724072	6.541229663
Mo26	6.413431106	9.396678911	1.56583724	6.413431106	9.396678911	1.56583724
Mo27	8.791390667	8.391709576	4.278345071	8.791390667	8.391709576	4.278345071
Mo28	5.451398697	2.005607244	6.697177384	5.455126305	2.009462967	6.696728625
Mo29	8.659464863	8.536083529	1.79659522	8.659464863	8.536083529	1.79659522
Mo30	7.914469664	3.425710964	6.160791531	7.915615547	3.422036272	6.153100583
Mo31	7.357905841	6.127618381	7.120654229	7.361409611	6.124480512	7.121292129
Mo32	5.889067877	5.350765513	4.994741171	5.889501602	5.352552167	4.993556928
Mo33	6.413431106	6.98880385	1.56583724	6.413431106	6.98880385	1.56583724
Mo34	8.507290471	5.915219936	4.718530213	8.508520066	5.913677635	4.709505938
C1	2.685191555	7.896579701	0.282436568	2.685191555	7.896579701	0.282436568
C2	1.863832091	5.253289161	2.564774511	1.863832091	5.253289161	2.564774511
C3	1.863832091	0.437539034	2.564774511	1.863832091	0.437539034	2.564774511
C4	2.685191555	3.066935895	0.241075186	2.685191555	3.066935895	0.241075186
C5	2.598818707	8.861996918	5.171332415	2.635823943	8.744443638	5.158667769
C6	1.742878469	6.355750856	7.225116324	1.745603354	6.338732791	7.2450846
C7	1.898789569	1.933987698	7.477739416	1.890862865	1.869340217	7.536100995
C8	2.779671422	4.613115348	4.617794325	2.779671422	4.613115348	4.617794325
N1	7.882404343	1.950046616	3.098603641	7.882404343	1.950046616	3.098603641
N2	5.624097078	0.661815156	3.067007082	5.624097078	0.661815156	3.067007082
N3	9.626350139	9.591137067	6.078046367	9.614631678	9.590329656	6.083815784
N4	5.645616511	8.912758193	6.069918104	5.651958602	8.906043524	6.064078212
N5	9.448606596	4.736764041	0.150798652	9.448606596	4.736764041	0.150798652
N6	7.203147904	3.684419794	0.064759583	7.203147904	3.684419794	0.064759583
N7	5.835816152	3.77788495	6.061220007	5.834663596	3.782348579	6.062210892
N8	9.448606596	9.552514163	0.150798652	9.448606596	9.552514163	0.150798652
N9	7.203147904	8.500169629	0.064759583	7.203147904	8.500169629	0.064759583
N10	7.882404343	6.765796452	3.098603641	7.882404343	6.765796452	3.098603641
N11	5.624097078	5.477564704	3.067007082	5.624097078	5.477564704	3.067007082

N12	9.1496542	4.87632558	6.528690308	9.154138249	4.874882586	6.528380695
H1	1.898789569	2.150588352	8.892564985	1.895819614	2.158816209	8.706443783

References

[1]H. Liu, J. Cheng, W. He, Y. Li, J. Mao, X. Zheng, C. Chen, C. Cui, Q, Appl. Catal. B-Environ. 304 (2022).

[2]Perdew, Burke, Phys. Rev. lett. 77 (1996) 3865-3868.

[3]<hammer1999.pdf>.

[4]J.K. Norskov, T. Bligaard, A. Logadottir, J.R. Kitchin, J.G. Chen, S. Pandelov, J.K. Norskov, J. Electrochem. Soc. 152 (2005) J23-J26.

[5]Y Liu, G Yu, GD Li, Y Sun, T Asefa, W Chen, X Zou, Angew. Chem. Int. Ed. Engl. 2015,54(37):10752-10757.

[6]Z Liu, S Zhou, S Xue, Z Guo, J Li, K Qu, W Cai, Chem. Eng. J. 2021,421.

[7]ZY Yu, Y Duan, MR Gao, CC Lang, YR Zheng, SH Yu, Chem. Sci. 2017,8(2):968-973.

[8]Y Zhang, H Zhou, H Wang, Y Zhang, DD Dionysiou, Chem. Eng. J. 2021,418.

[9]Q Wu, D Zhao, X Yu, J Xu, N Wang, W Zhou, L Li, Int. J. Hydrogen Energy. 2022,47(8):5064-5073.

[10]H Yang, X Chen, G Hu, WT Chen, SJ Bradley, W Zhang, G Verma, T Nann, DE Jiang, PE Kruger, X Wang, H Tian, GIN Waterhouse, SG Telfer, S Ma, Chem. Sci. 2020,11(13):3523-3530.

[11]L Ji, J Wang, X Teng, H Dong, X He, Z Chen, ACS Appl. Mater. Interfaces. 2018,10(17):14632-14640.

[12]A Mukherji, R Bal, R Srivastava, ChemElectroChem. 2020,7(13):2740-2751.

[13]M Li, Y Zhu, H Wang, C Wang, N Pinna, X Lu, Adv. Energy Mater. 2019,9(10).

[14]H Lin, Z Shi, S He, X Yu, S Wang, Q Gao, Y Tang, Chem. Sci. 2016,7(5):3399-3405.

[15]F Yuan, Z Liu, G Qin, Y Ni, Dalton Trans. 2020,49(42):15009-15022.

[16]D Wang, T Liu, J Wang, Z Wu, Carbon. 2018,139:845-852.

[17]Y Zhao, S Wang, H Liu, X Guo, X Zeng, W Wu, J Zhang, G Wang, J. Phys. Chem. Solids. 2019,132:230-235.

[18]W Liu, X Wang, F Wang, K Du, Z Zhang, Y Guo, H Yin, D Wang, Nat. Commun.

2021,12(1):6776.

[19]X. Zhang, Z. Zhu, X. Liang, F.-X. Ma, J. Zhang, Y. Tan, Z. Pan, Y. Bo, C.-M. Lawrence Wu, Chem. Eng. J. 408 (2021).

[20]Y.Y. Chen, Y. Zhang, W.J. Jiang, X. Zhang, Z. Dai, L.J. Wan, J.S. Hu, ACS Nano. 10 (2016) 8851-8860.

[21]N Han, S Luo, C Deng, S Zhu, Q Xu, Y Min, ACS Appl. Mater. Interfaces. 2021,13(7):8306-8314.